Attribution of human-induced dynamical and thermodynamical contributions in extreme weather events

2016 Environ. Res. Lett. 11 114009

(http://iopscience.iop.org/1748-9326/11/11/114009)

Environmental Research Letters

LETTER

Attribution of human-induced dynamical and thermodynamical contributions in extreme weather events

R Vautard[1,6], P Yiou[1], F Otto[2], P Stott[3], N Christidis[3], G J van Oldenborgh[4] and N Schaller[2,5]

[1] LSCE/IPSL, Laboratoire CEA/CNRS/UVSQ & Université Paris-Saclay, Orme des Merisiers, F-91191 Gif sur Yvette CEDEX, France
[2] Environmental Change Institute, University of Oxford, South Parks Road, Oxford OX1 3QY, UK
[3] UK Met Office Hadley Centre, FitzRoy Road, Exeter EX1 3PB, UK
[4] Koninklijk Nederlands Meteorologisch Instituut, 3730 AE De Bilt, The Netherlands
[5] Department of Physics, Atmospheric Oceanic and Planetary Physics, University of Oxford, Oxford OX1 3PU, UK
[6] Author to whom any correspondence should be addressed.

OPEN ACCESS

RECEIVED
26 April 2016

REVISED
8 July 2016

ACCEPTED FOR PUBLICATION
23 August 2016

PUBLISHED
2 November 2016

Keywords: event attribution, extreme events, climate change, extreme precipitation

Abstract

We present a new method that allows a separation of the attribution of human influence in extreme events into changes in atmospheric flows and changes in other processes. Assuming two data sets of model simulations or observations representing a natural, or 'counter-factual' climate, and the actual, or 'factual' climate, we show how flow analogs used across data sets can provide quantitative estimates of each contribution to the changes in probabilities of extreme events. We apply this method to the extreme January precipitation amounts in Southern UK such as were observed in the winter of 2013/2014. Using large ensembles of an atmospheric model forced by factual and counterfactual sea surface temperatures, we demonstrate that about a third of the increase in January precipitation amounts can be attributed to changes in weather circulation patterns and two thirds of the increase to thermodynamic changes. This method can be generalized to many classes of events and regions and provides, in the above case study, similar results to those obtained in Schaller *et al* (2016 *Nat. Clim. Change* **6** 627–34) who used a simple circulation index, describing only a local feature of the circulation, as in other methods using circulation indices (van Ulden and van Oldenborgh 2006 *Atmos. Chem. Phys.* **6** 863–81).

1. Introduction

Every extreme weather event is unique and the result of the interplay between specific atmospheric dynamics (large-scale flows) and other physical processes. For instance, large-scale persisting anticyclonic and stagnant air conditions are necessary for the development of summer heat waves. This provides high radiation heating of the ground and allows for the accumulation of heat over a period of several days to weeks. However the heat build-up during such conditions strongly depends on the state of soil moisture (Seneviratne *et al* 2010, Quesada *et al* 2012). In the mid-latitudes cold spells in winter are usually generated by blocking anticyclones (Rex 1950) leading to strong radiative cooling of the Earth surface in the absence of clouds and strong meridional circulations. Snow cover, and its interplay with radiation, modulates temperatures (Shongwe *et al* 2007, Orsolini *et al* 2013). For heavy precipitation events both the large-scale flow conditions (in particular sustained zonal flow in Europe) and the thermodynamic capacity of the atmosphere to hold water are necessary causes of the event.

Human-induced climate change will likely act on all these processes by modifying, on the one hand, large-scale flows, and on the other hand many physical processes such as the thermodynamic increase of water vapor, which will be respectively be referred to as 'dynamical' and 'thermodynamical' changes in the following. In the past decade, a number of methods to detect and attribute a human influence in the change of odds of extreme events have been developed (see Stott *et al* 2016 for a review). However methods generally focused on assessing the overall human imprint on the probabilities of extremes but not attempted to

assess the individual contributions through the driving processes separately. In particular, detection of changes in large-scale circulation inducing changes in the frequency of occurrence of extreme events is a challenge due to the weak signal of climate change in flows compared to natural variability in flows. This issue has only been addressed in a handful of very recent studies. For instance, van Haren *et al* (2013) looked at the circulation patterns associated with extreme winter precipitation in the Rhine basin and found that these have become more frequent. Horton *et al* (2015) showed that an increasing frequency of summer anticyclonic conditions have probably increased the number of heat waves, but could hardly find a signal in the winter season but over Central/Western Asia. In a recent model study, Schaller *et al* (2016) showed that a human-induced increase of persisting low sea-level pressure (SLP) North West of Scotland has probably increased the probability of heavy precipitation in the Southern UK such as witnessed in the winter 2013/2014. The influence of changes in large-scale circulation on several climate variables was evidenced by van Ulden and van Oldenborgh (2006) and Vautard and Yiou (2009), but extreme events were not considered in these studies.

By contrast, the influence of anthropogenic climate change on the thermodynamic component of extremes has been shown to have altered the frequency and magnitude of extreme weather events in a few more instances. By conditioning on the large-scale flow Yiou *et al* (2007) and Cattiaux *et al* (2009) showed how warm the fall and winter of 2006/2007 was compared to previous decades in similar flows, and how an increase in sea surface temperatures (SST) with a similar atmospheric flow increases such autumn warmth. Similarly, Cattiaux *et al* (2010) showed that the cold winter of 2009–2010 was actually warmer than expected during the second half of the 20th century, given the negative record of North-Atlantic Oscillation index. Again conditioning on the flow, Yiou and Cattiaux (2014) and Christidis and Stott (2015) showed that in a climate without human influence, flows encountered along the stormy winter of 2013–2014 would have led to slightly weaker extreme precipitation amounts. They also showed a weak signal in the increase of occurrence of the sustained southerly flows that were part of the cause of the large amounts. To our knowledge the study of Schaller *et al* (2016) is the only one comprehensively assessing the overall change in the odds of extreme precipitation while also assessing the relative contribution of a change in the large-scale flow and the change in thermodynamics. However the method used an index for circulations that was tailored to the case (the monthly mean sea level pressure at a carefully selected point), and described one specific feature of the flow, which was shown to be sensitive to the exact SST patterns (Haustein *et al* 2016). This calls for a more general method that would be applicable to other areas and types extreme events also, and would account for more flow characteristics.

Building on this specific case study we here develop a generic methodology to detect and attribute dynamical and thermodynamical contributions to changes in the probabilities of extreme events, due to changes in external forcings. This method generalizes the analysis of Schaller *et al* (2016). The approach uses the 'flow analog' methodology, which was initially developed for a number of meteorological problems and limited observational records (e.g. weather predictability Lorenz 1969; downscaling Zorita and Von Storch 1999). Applied to detection problems, flow analogs were first used by Yiou *et al* (2007) for thermodynamical changes and Vautard and Yiou (2009) for dynamical changes, without developed formalism.

2. General methodology

Current event attribution schemes consider a one-dimensional climate variable or index x characterizing the extreme event. This can be precipitation or temperature or a more complex index, including impact indicators such as river run-off or wet-bulb temperature. It is characterized over a certain temporal and spatial scale. In the example of the extreme rain amount of January 2014 developed by Schaller *et al* (2016), x is the monthly rainfall amount averaged over Southern UK Let us consider the 'extreme event' or the 'class of extreme events' as defined by 'x exceeding a certain threshold x_0'. Over the same time scale, the large-scale atmospheric flow F can be characterized by mean SLP or the 500 hPa geopotential height (Z500) field over a region which is characterizing the large scale weather pattern over the area of the extreme event. In previous studies over Europe (Yiou *et al* 2007, Cattiaux *et al* 2010), for instance, the Euro-Atlantic (30–65N, 80W–30E) region was selected. In this study, we focus on a smaller atmospheric region, used in the framework of the EURO-CORDEX project (Jacob *et al* 2014).

The relation between x and the flow is not unequivocal, but similar flows lead to a similar probability distributions of x, which can strongly deviate from the climatological distribution. We will call hereafter these probabilities the 'flow-conditioned probabilities', bearing in mind that these depend on the definition of the flow. For instance, van Ulden and van Oldenborgh (2006) showed how the PDFs of monthly mean temperature and precipitation in the Netherlands depend on the circulation characteristics. Christidis and Stott (2015) showed that the type of flows encountered during Winter 2013/2014 increased the probability of large amounts of precipitation in Southern UK (defined by DJF precipitation over Southern UK exceeding a threshold corresponding to a 1-in-10 yr event estimated with DJF rainfall data since 1948/49) by a factor of 8 relative to climatology. Similarly,

anticyclonic summer flows generally lead to a shifted temperature distribution, leading to an increased probability of exceeding a high temperature threshold relative to climatology in summer and low temperatures in winter. Here, as in previous articles (e.g. Cattiaux *et al* 2010), we calculate the flow-conditioned probabilities by counting empirically the frequency, among similar flows, of those leading to an exceedance. The similarity—or analogy—of flows is defined in two ways here: flow clusters or flow analogs.

The general methodology aims at decomposing the changes in probabilities of exceeding a threshold for x between two different 'worlds' representing the factual world with greenhouse gas and aerosol concentrations as observed today and a counterfactual world with the anthropogenic forcings removed. To estimate how changes in the flows alone have influenced exceedance probabilities, the key concept is to combine the counterfactual distribution of flows with the factual flow-conditioned probabilities, and to compare it with the combination of factual distribution of flows with factual flow-conditioned probabilities. This requires that one can calculate the factual flow-conditioned probability for each counterfactual flow. A main assumption here is therefore that we can find good analogs of each counter-factual flow in the factual set of flows. This is a reasonable assumption precisely because of the comparably small anthropogenic signal on the large-scale flow. To detect possible changes on the atmospheric circulation in the first place large ensembles of simulations and advanced statistics are necessary. If the two worlds were drastically different in obvious ways, then the exercise of detection and attribution would be trivial.

We now show how these concepts unfold using two similarity definitions, the first one (flow clusters) being conceptually simpler but less general than the second (analogs) for operational use.

2.1. Flow clusters

A simple way to define flow similarity is through gathering flows into a small number K of fixed clusters $F_1, F_2, \ldots, F_K$, or 'weather regimes' (Mo and Ghil 1987, Michelangeli *et al* 1995) according to a metric. The flow-conditioned probabilities of x are then calculated as fixed within a given cluster assuming that all flows within the cluster lead to identical distributions of x. The climatological probability $P(x > x_o)$ of x exceeding threshold x_o can be calculated as the average of the probability conditional on each specific cluster weighted by the cluster frequency:

$$P(x > x_o) = \sum_{k=1}^{K} P(x > x_o \,|F_k) P(F_k), \qquad (1)$$

where $P(x > x_o \,|F_k)$ are the individual flow-conditioned probabilities for the extreme event defined by exceeding threshold x_o, i.e. $P(x > x_o \,|F_k)$ is the probability of exceeding x_o in cluster F_k, with $P(F_k)$ being the probability of the flow falling in cluster F_k.

Following the above principles, we assume that the factual and counterfactual worlds have the same clusters, however with potentially different probabilities of occurrence. Thus, all probabilities in equation (1) can be different in the two different ensembles representing the factual world:

$$P_{\mathrm{f}}(x > x_o) = \sum_{k=1}^{K} P_{\mathrm{f}}(x > x_o|F_k) P_{\mathrm{f}}(F_k) \qquad (2)$$

and the counterfactual world that might have been with anthropogenic drivers removed:

$$P_{\mathrm{c}}(x > x_o) = \sum_{k=1}^{K} P_{\mathrm{c}}(x > x_o \,|F_k) P_{\mathrm{c}}(F_k). \qquad (3)$$

Since we assume that cluster types are the same in both worlds and that the probability of an extreme is constant within each cluster (but different in factual and counterfactual worlds), dynamical changes are exclusively due to changes in probabilities of occurrence of each flow type between the two cases, $P_{\mathrm{f}}(F_k)$ and $P_{\mathrm{c}}(F_k)$. The dynamical contribution of climate change on the threshold exceedance probability can be measured by replacing the factual with the counterfactual cluster occurrence probabilities in (2) and subtracting it from (2):

$$\begin{aligned} \Delta P_{\mathrm{dyn}}(x > x_o) \;=\; & \sum_{k=1}^{K} P_{\mathrm{f}}(x > x_o|F_k) \\ & .\,(P_{\mathrm{f}}(F_k) - P_{\mathrm{c}}(F_k)). \end{aligned} \qquad (4)$$

Similarly, effects of changes in other than dynamical processes, which will be called here 'thermodynamical changes contribution', can be estimated as:

$$\begin{aligned} \Delta P_{\mathrm{therm}}(x > x_o) \;=\; & \sum_{k=1}^{K} (P_{\mathrm{f}}(x > x_o|F_k) \\ & - P_{\mathrm{c}}(x > x_o|F_k)).\, P_{\mathrm{f}}(F_k). \end{aligned} \qquad (5)$$

Note that both contributions do not necessarily add up to the overall probability change $P_{\mathrm{f}}(x > x_o) - P_{\mathrm{c}}(x > x_o)$ due to remaining cross-terms:

$$\begin{aligned} P_{\mathrm{f}}(x > x_o) - P_{\mathrm{c}}(x > x_o) &= \Delta P_{\mathrm{dyn}}(x > x_o) \\ &+ \Delta P_{\mathrm{therm}}(x > x_o) + \sum_{k=1}^{K} (P_{\mathrm{f}}(x > x_o|F_k) \\ &- P_{\mathrm{c}}(x > x_o|F_k)).\,(P_{\mathrm{c}}(F_k) - P_{\mathrm{f}}(F_k)). \end{aligned} \qquad (6)$$

However these terms should be of second order and small if changes between factual and counter-factual are small as assumed. If not, this would mean either a drastic change in flows or in thermodynamics or both.

Figure 1 illustrates the above concepts from a synthetic example with four flow clusters. In Clusters #1 and #3 the probability of occurrence are equal in the two different ensembles, while Cluster #2 dominates in the counterfactual climate and Cluster #4 dominates in the factual climate. In Clusters #1 and #4, thermodynamical changes induce a higher probability of exceedance than in Clusters #2 and #3 where there is no thermodynamical change. In this example Cluster #3 does not undergo any change between the two climates, Cluster #1 changes are due

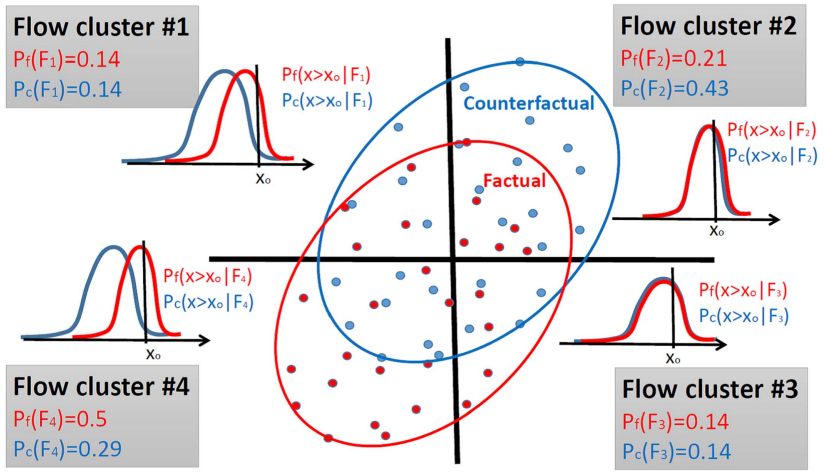

Figure 1. Synthetic example of discrete flow analysis of dynamical and thermodynamical of changes. Individual flows are represented by dots. Each point represents a flow in the 'phase space', clustered in one of the four regimes (the quadrants). All elements from factual climate are displayed in red color and counterfactual climate in blue color. The conditional PDFs are shown as well as the threshold x_o. See text for interpretation.

to thermodynamics only, Cluster #2 changes are due to dynamics only, and in Cluster #4, the probability of extreme events becomes higher both due to dynamics and thermodynamics. The overall probability of exceedance is higher in the factual climate, due to all contributions.

2.2. Flow analogs

In the above case, flow-conditioned probabilities are uniform within each flow cluster. While a few clusters can group 'analog' flows with grossly similar features, they aggregate weather patterns that can have quite different details, potentially hindering an accurate characterization of flow-conditioned event probabilities. To make flow-conditioned probabilities more specific to each flow F, $P(x > x_o\ |F)$ is now estimated by selecting a set of neighboring analogs F_k of F and empirically counting the frequency of x values corresponding to these analogs, exceeding the threshold in this set, and dividing by the number of analogs K:

$$P(x > x_o\ |F) = K_a/K, \tag{7}$$

where K is the number of closest flow analogs of F, using for instance the Euclidian distance among SLP fields over a specified domain, and K_a the number of analogs for which the corresponding value of x exceeds the threshold x_o. This analog approach in a sense generalizes the weather regime approach, considering one regime per distinct flow, instead of a small finite number of clusters comprising different flows. The remaining assumption is that the flow F is not so exceptional that there are no good analogs.

We now apply this to the attribution simulations as above. Assuming that one has at hand ensembles of N_f factual and N_c counterfactual simulated flows and climate indices x, and the ensembles are large enough, the overall probability of exceedance can be estimated as the average of individual flow-conditioned probabilities in each of the two ensembles (factual and counterfactual):

$$P_\mathrm{f}(x > x_o) = \frac{1}{N_\mathrm{f}}\sum_{n=1}^{N_\mathrm{f}} P_\mathrm{f}(x > x_o\ |F_{\mathrm{f},n}) \tag{8}$$

and

$$P_\mathrm{c}(x > x_o) = \frac{1}{N_\mathrm{c}}\sum_{n=1}^{N_\mathrm{c}} P_\mathrm{c}(x > x_o\ |F_{\mathrm{c},n}), \tag{9}$$

where $F_{\mathrm{f},n}$ and $F_{\mathrm{c},n}$ are the individual flows in the factual and counterfactual climate data sets.

To isolate the contribution of flow changes in passing from counterfactual to factual worlds, an 'intermediate' world can be conceptually designed where flows are the counterfactual flows and x is in the factual world.

Dynamical changes are estimated by subtracting from equation (8) the result obtained by using counterfactual flows, instead of factual flows, and searching their analogs in the factual flow ensemble:

$$\begin{aligned} P_\mathrm{dyn}(x > x_o) \;=\; & \frac{1}{N_\mathrm{f}}\sum_{n=1}^{N_\mathrm{f}} P_\mathrm{f}(x > x_o|F_{\mathrm{f},n}) \\ & - \frac{1}{N_\mathrm{c}}\sum_{n=1}^{N_\mathrm{c}} P_\mathrm{f}(x > x_o|F_{\mathrm{c},n}). \end{aligned} \tag{10}$$

Symmetrically, effects of thermodynamical changes are estimated by subtracting from equation (8) the result of using factual flows, and searching their counterfactual analogs to estimate the flow-conditioned probabilities:

$$\begin{aligned} P_\mathrm{therm}(x > x_o) \;=\; & \frac{1}{N_\mathrm{f}}\sum_{n=1}^{N_\mathrm{f}} P_\mathrm{f}(x > x_o|F_{\mathrm{f},n}) \\ & - \frac{1}{N_\mathrm{f}}\sum_{n=1}^{N_\mathrm{f}} P_\mathrm{c}(x > x_o|F_{\mathrm{f},n}). \end{aligned} \tag{11}$$

Note that we took here the factual world as the reference but equations similar to equations (10) and

(11) could have been derived taking the counterfactual climate as a reference (equation (9)). Tests showed that this would have given similar, albeit not equal results in the example below. However we prefer to have the factual climate as a reference as observation exist and uncertainty is therefore better controlled.

3. The example of extreme precipitation amount of January 2014 in Southern UK

We apply the methods described above to a very large ensembles of atmosphere-only general circulation simulations to disentangle dynamic and thermodynamic contributions of the increase in extreme January precipitation investigated in Schaller *et al* (2016). The experimental set-up uses about 17 000 model simulations of possible European winters in 2013/2014 for the factual climate, conditioned on the observed SST, and more than 100 000 simulations from 11 ensembles for the counterfactual climate, using observed SST patterns with the anthropogenic signal removed. Simulations use the factual and counterfactual climates were carried out using the HadAM3P atmospheric model, driven by prescribed SST and sea ice, and with a regional zoom over Europe and the eastern North Atlantic Ocean, at a spatial resolution of about 50 km. Initial conditions are perturbed slightly for each ensemble member on December 1. The patterns of warming removed from the SSTs in the counterfactual ensembles were calculated from 11 different CMIP5 model simulations were calculated by difference between the historical all-forcing simulations and the natural-forcing simulations. These ensembles were selected in order to account for uncertainty of the ocean warming attributable to the atmospheric composition.

Schaller *et al* (2016) estimated the contribution of flow changes by resampling factual monthly amounts of precipitation in bins of a very simple flow index, the mean SLP value North-West of Scotland [20W; 60N] (the point with strongest correlation with South UK precipitation), to match the distribution of counterfactual values of the index. This method is a simplified form of the method of van Haren *et al* (2013), and gives an easy way to compute estimation of the dynamical contribution to the overall change in the likelihood of high precipitation to occur but is strongly dependent on the exact MSLP response to SST patterns as shown by Haustein *et al* (2016). The method however only accounts for one local feature of the flow. Here we apply the formalism introduced above which takes into account the full SLP field over the regional area simulated by the HadAM3P model and hence is less dependent on the exact index chosen. Flows are characterized by monthly mean SLP fields taken over the regional domain (NE Atlantic and Europe), and the climate index is the monthly precipitation amount over Southern UK as in Schaller *et al* (2016).

In figure 2(a), the two exceedance probability distributions $P_f(x > x_o)$, $P_c(x > x_o)$, calculated from analogues and equations (8) and (9) are displayed for only one of the 11 ensembles (calculated from the GFDL-CM3 model), in the form of a return value versus return period diagram. In each case, a constant number of analogs (50) was used to estimate flow-conditioned probabilities in equations (8) and (9). Results are quite insensitive to the exact number of analog flows as shown below.

For this specific ensemble, the probability of a one-in-100-year event in the factual world is about 20% less without human influence. About half of this decrease is due to dynamical changes only, as obtained by replacing factual flows by counterfactual flows but using the same conditional probabilities given the flows (equation (10)). Thus in a climate with counterfactual dynamical structures and factual thermodynamics the probability of extreme precipitation amount is about 10% less than in the factual climate.

The estimation of the exceedance probabilities $P_f(x > x_o)$ and $P_c(x > x_o)$ were calculated from equations (8) and (9) using analogs but can also be directly calculated by counting the number of exceedances in the two ensembles. Results are also shown in figure 2(a) (dotted red and blue curves). Direct estimations slightly differ (by about 5%–10%) from analog estimations, a fact that can be explained by the imperfect nature of flow analogs.

The average results from the 11 ensembles are shown in figure 2(b). For one-in-100-year events, we find that human influence induces an average increase of about 40% of the probability of extreme January precipitation amount in Southern UK, or equivalently that the risk is reduced by about 30% without human influence relative to the actual world. A climate with factual thermodynamics and counterfactual flows would have about 10% less extremes than the factual climate, explaining about a third of the human influence. Thermodynamical changes explain the other two thirds of the changes (figure 2(b)), as obtained by searching analogs of factual flows in the counterfactual simulations set.

We found different results when using the flow cluster method as described in equations (2)–(5). In this case the flow clustering method is based on daily SLP over the North-Atlantic as described in Schaller *et al* (2016), providing four weather types as in previous studies (Michelangeli *et al* 1995). For details of the method and cluster results the reader is referred to (Schaller *et al* 2016). Each daily flow of each simulation was given a cluster number, and monthly flow clusters were defined as the most populated daily cluster in the month. The average contribution of dynamical changes is much weaker (see figures 2(b) and (d)). This is not surprising as the flow-conditioned probabilities are constant within each cluster, having thousands of

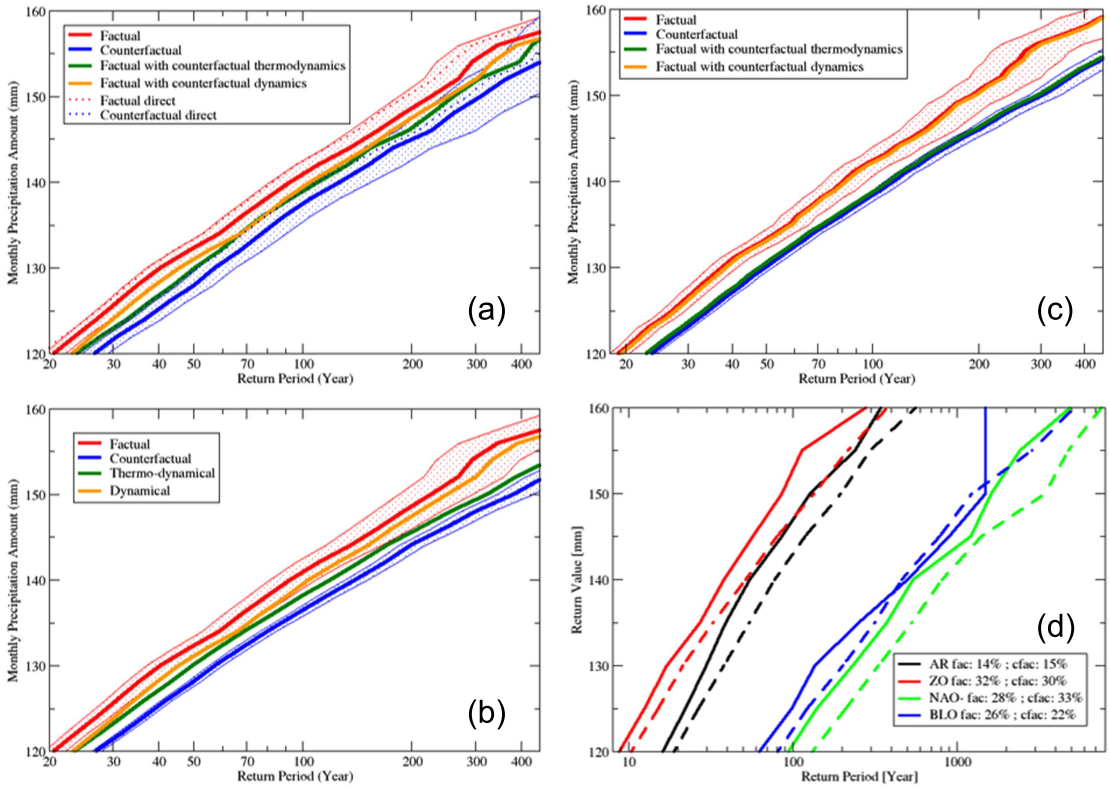

Figure 2. Top left (a): return values as a function of return periods for the probabilities of exceedance $P_f\,(x > x_o)$ (red solid), $P_c\,(x > x_o)$ (blue solid), and the probabilities obtained by replacing factual by counterfactual flows while keeping the factual flow-conditioned probabilities (orange solid) and vice versa (factual flows with counterfactual flow-conditioned probabilities, green solid) for one of the counterfactual ensemble of simulations. More than 17 000 winters were simulated for the factual climate and more than 15 000 simulations for the counterfactual climate. 5%–95% ranges on probabilities (red and blue shading) are calculated by the probability $\pm 2\sqrt{p(1-p)/n}$, where n is the number of degrees of freedom, taken here as the number of independent simulations, p is the exceeance probability, and bounds are then transformed into return period. Bottom left (b): same as top left but averages of probabilities across the 11 ensembles is taken for the counterfactual climate. Right panel (c): same as (b) but using the flow cluster method; right bottom panel (d): flow-conditioned probabilities obtained for each weather regime (cluster). For this panel, factual: solid lines; counterfactual: dashed lines; flow regime names, and their occurrence frequencies in each set of simulations are indicated in the legend.

different flows, while only the 50 best analogs are selected with the analog method. This makes the flow-conditioned probabilities (thermodynamics) much less flow specific. In addition, the wettest regimes (AR and ZO, see figure 2(d)), have opposite frequency changes from factual to counterfactual worlds (figure 2(d), legend). Note in particular that the wettest regime, ZO is slightly more frequent in the counterfactual than in the factual climate. This may seem contradictory with the Schaller *et al* (2016) finding of more frequent very low pressure values at [60W; 20N] (see their figure 4(c)). The discrepancy relies on the definitions of the flow, more specific in the pressure index case.

The relative dynamical and thermodynamical contributions, calculated in % as

$$100.P_{\mathrm{dyn}}\,(x > x_o)/(P_f\,(x > x_o) - P_c\,(x > x_o))$$

and

$$100.P_{\mathrm{therm}}\,(x > x_o)/(P_f\,(x > x_o) - P_c\,(x > x_o))$$

using equations (10) and (11) are shown as a function of the precipitation amount threshold in figure 3(a). We find that the dynamical contribution decreases for more extreme precipitations, but the significance of this trend is hard to estimate. Notice that the two contributions almost add up to 100%, which results from similar considerations as those for equation (6). This confirms the validity of our assumption of not-too-different worlds, at least for this example.

In order to test the robustness of the results to the parameters of the method we reproduced figure 3(a) but changing (i) the number of analogs and (ii) the distance to measure analogy of flows. The number of analogs was decreased to 10 (figure 3(b)) and increased to 500 (figure 3(c)) instead of 50. Instead of the 'flat' Euclidian distance, a distance with spatial weights proportional to the square of the correlation between monthly precipitation amounts and SLP was used in order to optimize the relation between atmospheric circulation and precipitation (figure 3(d)). The average results are quite insensitive to these methodological changes, showing the robustness of the approach. In each case, the change in large-scale dynamical flow explain a fraction between 20% and 50% of the change in the probability of extreme precipitation amount, decreasing as a function of precipitation intensity. The

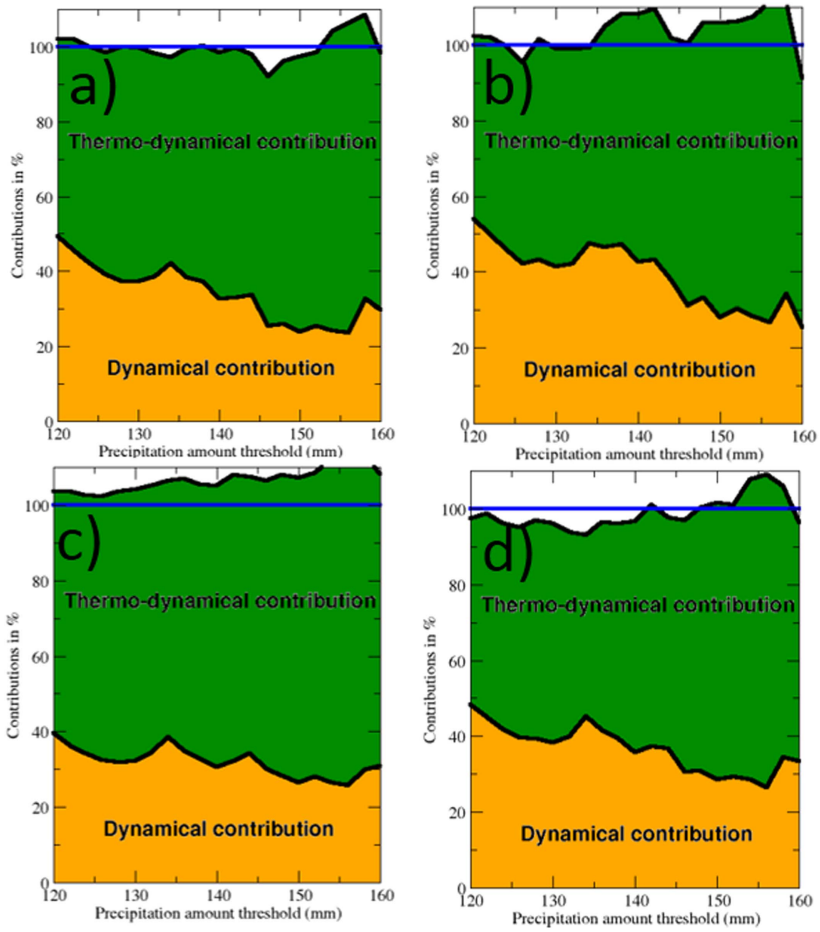

Figure 3. (a) Cumulated dynamical and thermodynamical contributions, in % of the difference between factual and counterfactual overall probabilities. (b) Same as (a) for experiments where the parameters of the method are changed: left panel: 10 best analogs instead of 50; (c) same as in (a) with 500 best analogs instead of 50; (d) same as in (a) but with a change in the distance used to identify the 50 best analogs. The distance is weighted by the square of the pointwise correlation between the monthly precipitation and the SLP.

trend toward a larger contribution of thermodynamics for more extreme cases is found in all experiments.

4. Discussion

We have presented two methods for disentangling the dynamical and thermodynamical contributions of changes in the likelihood of occurrence of extreme weather events due to external drivers within the framework of probabilistic extreme event attribution. The first method uses a classification of weather types and estimates separately changes in cluster frequency and conditional probability of extreme events within each cluster and combines them to estimate the dynamical and thermodynamical contributions to attributed changes between ensembles of factual and counterfactual climate simulations. The other method estimates flow-conditioned extreme event probabilities using analogs of individual flows simulated in factual or in counterfactual ensembles. When applied to extreme precipitations in Southern UK, we find that about a third of the change in risk is attributable to atmospheric flow changes, using the analog method. Despite a very different and more general method, we found results similar to those of Schaller *et al* (2016). The method developed here accounts for the multi-dimensional nature of the flow. The results obtained using a few clusters are found to be different, with a lower dynamical contribution, which can be explained by the loose characterization of flows using only a few clusters.

This method calls for a number of further developments and applications, as well as an evaluation for different types of extreme events. Here we used only model data presented in large ensembles. Using observations, instead, is more difficult due to the much more limited number of samples. However previous studies using flow analogs (see e.g. Cattiaux *et al* 2010) showed that such application should be possible. Factual and counterfactual data sets can be represented by analyzing different time slices in the observation data sets. Sufficiently accurate reanalyses or observational data sets are now available since the middle of the last century, allowing the split into two 30 year long periods. The difference between factual and counterfactual climates in this case cannot be directly

interpreted as human influence, as many other processes (such as long-term natural variability) enter into play during this periods. While monthly or seasonal analogs such as calculated here are not possible due to insufficient number of samples, shorter events could be studied. Other types of extremes can also be investigated. Such applications are currently being developed such as for the attribution of the extremely warm winter of 2015.

The method developed here is quite generic and not designed to study only the attribution of human influence on climate change. The separation of factual and counterfactual ensembles can also be done on the basis of other external drivers (e.g. SST anomalies, El Niño years, different aerosol forcings). In principle it can also be used to analyse other indices than classical climate variables, or even impact indices.

While one can expect the method to be applicable in theory to both extratropical and tropical extreme phenomena, it is however less clear how results can be interpreted for tropical phenomena such as extreme precipitations or even heat waves. In the tropics, flows are very much influenced themselves by thermodynamical conditions so the interpretation of the dynamical/thermodynamical split should account for this.

It is important to stress that the method applies to the attribution of 'classes of events', where the observed event is used to define the class of events, often identified as exceedance of a threshold (e.g., Rahmstorf and Coumou 2011 for the Russian heatwave 2010), and not attribution studies of specific events (e.g., Dole *et al* 2011 for the Russian heatwave 2010). Similar to the majority of attribution studies (e.g. Herring *et al* 2015), the definition of the event or class of events in our study does not include other parameters than the meteorological variable causing the impacts with the SST anomaly being the only conditioning factor here. If other framings of event attribution studies are considered such as the event being defined as the conjunction of an impacting variable together with the flow itself, or other variables (e.g., Hannart *et al* 2015) the methodology would need to be extended to such cases.

The method of disentangling the dynamical and thermodynamical contributions introduced here aims at producing rather fundamental elements for explaining the mechanisms of climate change. However, detailing the processes involved in human influence on climate is always attractive for the public. Provided available observations, or pre-calculated model simulations can be used in near-real time, calculations performed here can easily be automated and applied to provide explanations of weather events and their links to climate change in a time frame of a few days after the events, making it possible to provide scientific evidence while the event is discussed in the media.

Acknowledgments

This study was conducted in the framework of the EUCLEIA (EUropean Climate and weather Events: Interpretation and Attribution) project under the European Union's Seventh Framework Programme [FP7/2007-2013] under grant agreement n° 607085'. It was also supported by the French Ministry of ecology within the framework of the 'EXTREMOSCOPE' project. P Yiou was also supported by the ERC Grant No. 338965-A2C2.

References

Cattiaux J, Vautard R, Cassou C, Yiou P, Masson-Delmotte V and Codron F 2010 Winter 2010 in Europe: a cold extreme in a warming climate *Geophys. Res. Lett.* **37** L20704

Cattiaux J, Vautard R and Yiou P 2009 Origins of the extremely warm European fall of 2006 *Geophys. Res. Lett.* **36** L06713

Christidis N and Stott P A 2015 Extreme rainfall in the United Kingdom during winter 2013/14: the role of atmospheric circulation and climate change *Bull. Am. Meteorol. Soc.* **96** S46–50

Dole R, Hoerling M, Perlwitz J, Eischeid J, Pegion P, Zhang T and Murray D 2011 Was there a basis for anticipating the 2010 Russian heat wave? *Geophys. Res. Lett.* **38** L06702

Hannart A, Pearl J, Otto F E L, Naveau P and Ghil M 2015 Causal counterfactual theory for the attribution of weather and climate-related events *Bull. Am. Meteorol. Soc.* (doi: 10.1175/BAMS-D-14-00034.1)

Haustein K, Otto F E L, Uhe P, Schaller N, Allen M R, Hermanson L, Christidis N, McLean P and Cullen H 2016 Real-time extreme weather event attribution with forecast seasonal SSTs *Environ. Res. Lett.* **11** 064006

Herring S C, Hoerling M P, Kossin J P, Peterson T C and Scott P A 2015 Explaining extreme events of 2014 from a climate perspective *Bull. Am. Meteorol. Soc.* **96** S1–172

Horton D E, Johnson N C, Singh D, Swain D L, Rajaratnam B and Diffenbaugh N S 2015 Contribution of changes in atmospheric circulation patterns to extreme temperature trends *Nature* **522** 465–9

Jacob D *et al* 2014 EURO-CORDEX: new high-resolution climate change projections for European impact research *Reg. Environ. Change* **14** 563–78

Lorenz E N 1969 Atmospheric predictability as revealed by naturally occurring analogues *J. Atmos. Sci.* **26** 636–46

Michelangeli P A, Vautard R and Legras B 1995 Weather regimes: recurrence and quasi stationarity *J. Atmos. Sci.* **52** 1237–56

Mo K C and Ghil M 1987 Statistics and dynamics of persistent anomalies *J. Atmos. Sci.* **44** 877–902

Orsolini Y J, Senan R, Balsamo G, Doblas-Reyes F J, Vitart F, Weisheimer A, Carrasco A and Benestad R E 2013 Impact of snow initialization on sub-seasonal forecasts *Clim. Dyn.* **41** 1969–82

Quesada B, Vautard R, Yiou P, Hirschi M and Seneviratne S I 2012 Asymmetric European summer heat predictability from wet and dry southern winters and springs *Nat. Clim. Change* **2** 736–41

Rahmstorf S and Coumou D 2011 Increase of extreme events in a warming world *Proc. Natl Acad. Sci.* **108** 17905–9

Rex D F 1950 Blocking action in the middle troposphere and its effect upon regional climate *Tellus* **2** 275–301

Schaller N *et al* 2016 Human influence on climate in the 2014 Southern England winter floods and their impacts *Nat. Clim. Change* **6** 627–34

Seneviratne S I, Corti T, Davin E L, Hirschi M, Jaeger E B, Lehner I and Teuling A J 2010 Investigating soil moisture–climate interactions in a changing climate: a review *Earth-Sci. Rev.* **99** 125–61

Shongwe M E, Ferro C A, Coelho C A and Jan van Oldenborgh G 2007 Predictability of cold spring seasons in Europe *Mon. Weather Rev.* **135** 4185–201

Stott P *et al* 2016 Attribution of extreme events *WIRES Clim. Change* **7** 23–41

van Haren R, van Oldenborgh G J, Lenderink G and Hazeleger W 2013 Evaluation of modeled changes in extreme precipitation in Europe and the Rhine basin *Environ. Res. Lett.* **8** 014053

van Ulden A P and van Oldenborgh G J 2006 Large-scale atmospheric circulation biases and changes in global climate model simulations and their importance for climate change in Central Europe *Atmos. Chem. Phys.* **6** 863–81

Vautard R and Yiou P 2009 Control of recent European surface climate change by atmospheric flow *Geophys. Res. Lett.* **36**

Yiou P and Cattiaux J 2014 Contribution of atmospheric circulation to wet Southern European winter of 2013 *Bull. Am. Meteorol. Soc.* **95** S66–9

Yiou P, Vautard R, Naveau P and Cassou C 2007 Inconsistency between atmospheric dynamics and temperatures during the exceptional 2006/2007 fall/winter and recent warming in Europe *Geophys. Res. Lett.* **34**

Zorita E and Von Storch H 1999 The analog method as a simple statistical downscaling technique: comparison with more complicated methods *J. Clim.* **12** 2474–89